Organometallics **1983**, *2*, 1635–1639

Unidentate Diphosphine Complexes. Crystal Structure and Molecular Geometry of $Fe(CO)_4(\eta^1\text{-}PPh_2CH_2CH_2PPh_2)$

Richard L. Keiter,*[1a] Arnold L. Rheingold,*[1b] Julian J. Hamerski,[1a] and Charles K. Castle[1a]

Departments of Chemistry, Eastern Illinois University, Charleston, Illinois 61920, and University of Delaware, Newark, Delaware 19711

Received June 14, 1983

The unidentate diphosphine complexes $Fe(CO)_4(\eta^1\text{-}PPh_2CH_2CH_2PPh_2)$ and *trans*-$Fe(CO)_3(\eta^1\text{-}PPh_2CH_2CH_2PPh_2)_2$ have been prepared by base-promoted addition of PPh_2H to $Fe(CO)_4(PPh_2CH{=}CH_2)$ and *trans*-$Fe(CO)_3(PPh_2CH{=}CH_2)_2$, respectively. The crystal structure and molecular geometry of $Fe(CO)_4(\eta^1\text{–}PPh_2CH_2CH_2PPh_2)$ have been determined by X-ray diffraction techniques. The compound crystallizes in the monoclinic space group $P2_1/c$ with $a = 8.518$ (3) Å, $b = 21.897$ (6) Å, $c = 14.341$ (3) Å, and $\beta = 93.74$ (3)°. The geometry about iron is trigonal bipyramidal with one end of the diphosphine bonded axially. $^{31}P\{^1H\}$ NMR shows that phosphorus–phosphorus coupling through the metal in *trans*-$Fe(CO)_3(\eta^1\text{-}PPh_2CH_2CH_2PPh_2)_2$ is relatively small (30.4 Hz).

Introduction

Bridged and chelated complexes of $PPh_2CH_2CH_2PPh_2$ (diphos) have been known for nearly as long as the ligand itself.[2] Unidentate diphos complexes are much rarer and in general have been synthesized unintentionally rather than by design. Solution spectroscopic characterization of $Co(NO)(CO)_2$ (η^1-diphos) appeared early on[3] and was followed by isolation of $Mn(\eta^5\text{-}C_5H_5)(CO)(NO)(\eta^1\text{-diphos})^+$,[4] $Co(\eta^1\text{-diphos})(\eta^2\text{-diphos})(CN)_2$,[5] and $Fe(\eta^5\text{-}C_5H_5)(CO)_2(\eta^1\text{-diphos})^+$.[6] These and other unidentate examples such as $M(CO)_5(\eta^1\text{-diphos})$ (M = Cr, Mo, W),[7] $[V(CO)_5\eta^1\text{-diphos}]^-$,[8] $Mo(\eta^5\text{-}C_5H_5)(\eta^1\text{-diphos})_2[C{=}C(CN)_2]Cl$,[9] Ru(porphyrin)$(\eta^1\text{-diphos})_2$,[10] $Fe_3Te_2(CO)_9(\eta^1\text{-diphos})$,[11] and $(\eta^5\text{-}C_5H_5)Fe(CO)H(\eta^1\text{-diphos})$[12] were synthesized by substitution reactions. The tendency for bridged or chelated diphos species to form in most of these reactions limits their usefulness. A method that eliminates these tendencies involves the addition of PPh_2H to coordinated vinyl phosphines and has been shown to be quite effective in the synthesis of group 6 complexes such as $M(CO)_5(\eta^1\text{-diphos})$ and $M(CO)_4(\eta^1\text{-diphos})_2$.[13] Until now the approach has not been applied to other transition-metal groups, and thus the scope of the reaction is unknown. In this paper we demonstrate that it is effective for the preparation of $Fe(CO)_4(\eta^1\text{-diphos})$ and $Fe(CO)_3(\eta^1\text{-diphos})_2$. As no unidentate diphos complexes have been subjected previously to X-ray analysis, we have determined the crystal structure and molecular geometry of $Fe(CO)_4(\eta^1\text{-diphos})$. We have also synthesized $Fe(CO)_4(\eta^1\text{-}PPh_2CH_2PPh_2)$ for comparative purposes.

Experimental Section

General Information. All reactions were carried out under an atmosphere of dry N_2. THF was purified by distillation from benzophenone ketyl. The phosphines and metal carbonyls were obtained from commercial sources and used without purification. Known procedures were used for the preparation of $W(CO)_5PPh_2H$,[13,14] $Fe(CO)_4PPh_2H$, and $Fe(CO)_3(PPh_2H)_2$.[15]

Infrared spectra were recorded on a Perkin-Elmer 337 spectrometer and expanded with a Beckman recorder. $^{31}P\{^1H\}$ NMR spectra were recorded at 40.5 MHz on a Varian XL-100 spectrometer. Chemical shifts are relative to external 85% phosphoric acid (downfield is positive). Melting points are uncorrected and were obtained with a Thomas-Hoover Unimelt apparatus. Microanalysis were carried out by Galbraith Laboratories or by the School of Chemical Sciences of the University of Illinois at Urbana.

$Fe(CO)_4PPh_2CH{=}CH_2$. A THF solution of sodium benzophenone ketyl was added to a THF solution of $PPh_2CH{=}CH_2$ and $Fe(CO)_5$. The product was isolated as described by Butts and Shriver (54%).[16] The product was also obtained by stirring a slight excess of $Fe_2(CO)_9$ with $PPh_2CH{=}CH_2$ at room temperature in toluene for 24 h (42%):[17] mp 55–56 °C; IR ($CHCl_3$) 2054, 1979, 1946 cm^{-1}, (C_6H_{12}) 2055, 1981, 1946 cm^{-1}; $^{31}P\{^1H\}$ NMR δ 66.5. Anal. Calcd for $C_{18}H_{13}O_4PFe$: C, 56.87; H, 3.45; P, 8.15. Found: C, 57.0, H, 3.58; P, 7.95.

$Fe(CO)_4(\eta^1\text{-}PPh_2CH_2PPh_2)$.[18] The sodium benzophenone ketyl method described above gave this complex in 71% yield:[16] IR (C_6H_{12}) 2046, 1980, 1948, 1936 cm^{-1}; $^{31}P\{^1H\}$ NMR δ_{PFe} 65.9, δ_{PC} −25.7 ($^2J_{PP}$ = 75.7 Hz).

***trans*-$Fe(CO)_3(PPh_2CH{=}CH_2)_2$.** Iron pentacarbonyl and $PPh_2CH{=}CH_2$ in THF were treated with $NaBH_4$ as described by Siegl[19] to give the complex (55%): decomp pt 170–172 °C; IR ($CHCl_3$) 1986 (s), 1941 (vw) cm^{-1}, (C_6H_{12}) 1884 (s), 1939 (vw) cm^{-1}; $^{31}P\{^1H\}$ NMR δ 75.9. Anal. Calcd for $C_{32}H_{26}P_2O_3Fe$: C, 65.97; H, 4.65; P, 10.98. Found: C, 65.65; H, 4.78; P, 10.75.

$Fe(CO)_4(\eta^1\text{-}PPh_2CH_2CH_2PPh_2)$. A solution of $Fe(CO)_4PPh_2CH{=}CH_2$ (2.7 mmol) in THF (25 mL) was added to

---

(1) (a) Eastern Illinois University. (b) University of Delaware.

(2) Chatt, J.; Hart, F. A. *Chem. Soc.* **1960**, 1378

(3) Mawby, R. J.; Morris, D.; Thorsteinson, E. D.; Basolo, F. *Inorg. Chem.* **1966**, *5*, 27.

(4) King, R. B.; Efraty, A. *Inorg. Chem.* **1969**, *8*, 2374.

(5) Rigo, P.; Longato, B.; Fevero, G. *Inorg. Chem.* **1972**, *11*, 300. Rigo, P.; Bressan, M.; Corain, B.; Turco, A. *J. Chem. Soc., Chem. Commun.* **1970**, 598.

(6) Brown, M. L.; Meyer, T. J.; Winterton, N. *J. Chem. Soc., Chem. Commun.* **1971**, 309.

(7) Keiter, R. L.; Shah, D. P. *Inorg. Chem.* **1972**, *11*, 191. Connor, J. A.; Day, J. P.; Jones, E. M.; MeEwen, G. K. *J. Chem. Soc., Dalton Trans.* **1973**, 347. Taylor, R. C.; Keiter, R. L.; Cary, L. W. *Inorg Chem.* **1974**, *13*, 1928. Grim, S. O.; Del gaudio, J.; Molenda, R. P.; Tolman, C. A.; Jesson, J. P. *J. Am. Chem. Soc.* **1974**, *96*, 3416.

(8) Fjare, K. L.; Ellis, J. E. *Organometallics* **1982**, *1*, 1373. Ellis, J. E.; Palazzotto, M. C. *J. Am. chem. Soc.* **1976**, *98*, 8264. Davison, A.; Ellis, J. E. *J. Organomet. Chem.* **1971**, *31*, 239.

(9) King, R. B.; Saran, M. S. *J. Am. Chem. Soc.* **1973**, *95*, 1817.

(10) Ball, R. G.; Domazetis, G.; Dolphin, D.; James, B. R.; Trotter, J. *Inorg. Chem.* **1981**, *20*, 1556.

(11) Lesch, D. A.; Rauchfuss, T. B. *Organometallics* **1982**, *1*, 499.

(12) Davies, S. G.; Hibberd, J.; Simpson, S. J. *J. Chem. Soc., Chem. Commun.* **1982**, 1404.

(13) Keiter, R. L.; Sun, Y. Y.; Brodack, J. W.; Cary, L. W. *J. Am. Chem. Soc.* **1979**, *101*, 2638.

(14) Strohmeier, W.; Müller, F. *Chem. Ber.* **1969**, *102*, 3608.

(15) Smith, J. G.; Thompson, D. T. *J. Chem. Soc.* **1967**, 1694.

(16) Butts, S. B.; Shriver, D. F. *J. Organomet. Chem.* **1979**, *169*, 191.

(17) Treichel, P. M.; Dean, W. K.; Douglas, W. M. *Inorg. Chem.* **1972**, 11, 1609.

(18) This complex was reported previously as a minor product (16%) from the photolysis of $Fe(CO)_5$ and $PPh_2CH_2PPh_2$: Wegner, P. A.; Evans, L. F.; Haddock, J. *Inorg. Chem.* **1975**, *14*, 192.

(19) Siegl, W. O. *J. Organomet. Chem.* **1975**, *92*, 321.

0276-7333/83/2302-1635$01.50/0

Table I. Crystal and Refinement Data

formula	$C_{30}H_{24}FeO_4P_2$
space group	$P2_1/c$ [C_{2h}^5, No. 14]
a, Å	8.518 (3)
b, Å	21.897 (6)
c, Å	14.341 (3)
β, deg	93.74 (3)
V, Å^3	2669.0 (14)
mol wt	566.24
ρ(calcd), g cm^{-3}	1.41
temp, °C	23
cryst dimens, mm	0.10 × 0.28 × 0.51 mm
radiation	graphite-monochromated Mo Kα (λ = 0.710 73 Å)
diffractometer	Nicolet R3
abs coeff, cm^{-1}	7.14
scan speed, deg/min	variable, 3.0–15.0
2θ scan range, deg	$3° \leqslant 2\theta \leqslant 45°$
scan technique	$\theta/2\theta$
data collected	$\pm h, +k, +l$
scan width, deg	$2.0 + \Delta(\alpha - \alpha_2)$
ignorance factor (g)[a]	0.0017
unique data	3509 rflns (3794 collected)
unique data with $(F_o)^2 > 2\sigma(F_o)^2$	2693
std rflns	3/144 (no decay obsd)
R_F	5.47
R_{wF}	5.49

[a] Weight = $[\sigma^2(F) + g(F^2)]^{-1}$.

PPh_2H (2.9 mmol) in THF (25 mL). After addition of potassium *tert*-butoxide (0.1 g), the mixture was heated at reflux for 2 h. The solvent was removed, and the crude mass was dissolved in a minimum of CH_2Cl_2. An equal volume of CH_3OH was added, and the crystalline product was collected after 12 h at 5 °C. (65%). The product was also prepared by heating a mixture of $Fe(CO)_4PPh_2CH{=}CH_2$ (2.7 mmol) and PPh_2H (2.9 mmol) in the presence of 2,2′-azobis(isobutyronitrile) (AIBN) without solvent for 8 h at 65 °C: mp 131–132°C; IR ($CHCl_3$) 2052, 1979, 1943 cm^{-1}, (C_6H_{12}) 2052, 1980, 1947, 1939 cm^{-1}; $^{31}P\{^1H\}$ NMR δ_{PFe} 68.1, δ_{PC} −13.1 ($^3J_{PP}$ = 40.2 Hz). Anal. Calcd for $C_{30}H_{24}O_4P_2Fe$: C, 63.62; H, 4.28. Found: C, 63.81; H, 4.46.

$Fe(CO)_3(\eta^1\text{-}PPh_2CH_2CH_2PPh_2)_2$. The base-promoted reaction described above was employed with a 2:1 ratio of PPh_2H to $Fe(CO)_3(PPh_2CH{=}CH_2)_2$ (79%) while free radical conditions gave 43%: mp 162–164 °C; IR ($CHCl_3$) 1886 (s), 1967 (vw) cm^{-1}, (C_6H_{12}) 1881 (s), 1892 (s), 1961 (vw) cm^{-1}; $^{31}P\{^1H\}$ NMR δ_{PFe} 76.4, δ_{PC} −14.1 ($^2J_{PP}$ = 30.4 Hz, $^3J_{PP} + {}^5J_{PP}$ = 49.1 Hz). Anal. Calcd for $C_{55}H_{48}O_3P_4Fe$: C, 70.55; H, 5.13; Fe, 5.96. Found: C, 70.91; H, 5.41; Fe, 5.00.

$(OC)_4FePPh_2CH_2CH_2PPh_2W(CO)_5$. A THF (40 mL) solution of $Fe(CO)_4PPh_2CH{=}CH_2$ (1.4 mmol), $W(CO)_5PPh_2H$ (1.4 mmol), and KO-*t*-Bu (0.08 g) was heated at reflux for 3 h. After the solution volume was reduced by three-fourths, CH_3OH (10 mL) was added to give product after 12 h at 5 °C: decomp pt 193–195 °C; IR ($HCCl_3$) 2076, 2054, 1982, 1941 cm^{-1}, (C_6H_{12}) 2073, 2053, 1981, 1953, 1940 cm^{-1}; $^{31}P\{^1H\}$ δ_{PFe} 68.9, δ_{PW} 12.5 ($^3J_{PP}$ = 42.8 Hz, J_{WP} = 240.7 Hz). Anal. Calcd for $C_{33}H_{24}P_2FeWO_9$: C, 47.21; H, 2.72; P, 6.96; Fe, 6.27. Found: C, 46.73; H, 2.75; P, 6.93; Fe, 5.62.

Collection and Processing of Diffraction Data. Details of intensity data collection and refinement procedures are provided in Table I. The centrosymmetric monoclinic space group $P2_1/c$ was uniquely indicated by the systematic absenses $h0l$ for $l = 2n + 1$ and $0k0$ for $k = 2n + 1$. All crystallographic computations were performed on the University of Delaware Data General Nova 4 computer using data collection, solution, and refinement programs contained in the Nicolet P3 and SHELXTL (version 3.0) program package. Corrections to the data for Lorentz and polarization effects were applied to the data. An empirical absorption correction based upon ψ scan data had a negligible effect on the final parameters of refinement as expected from the relatively low absorption coefficient (μ = 7.14 cm^{-1}) for this compound. Redundant and equivalent data were averaged ($R(I)$ = 2.79%).

Solution and Refinement of the Structure. The location of the iron and phosphorus atoms were obtained from the solution of highest combined figures of merit obtained from the direct methods routine SOLV. The remaining non-hydrogen atoms were located from subsequent difference Fourier syntheses. All non-hydrogen atoms were refined with anisotropic thermal parameters. Hydrogen atoms were placed in idealized positions (d(C–H) = 0.96 Å) and assigned isotropic thermal parameters 20% greater than the carbon atoms to which they were attached. A "riding" model was utilized to continuously update hydrogen atom positions during each refinement cycle. The final residuals were R_F

Table II. Final Positional Parameter for $(CO)_4Fe[(C_6H_5)_2PCH_2]_2$

atom	x	y	z	atom	x	y	z
Fe	−42 (1)	1817 (1)	4602 (1)	C(41)	−983 (7)	315 (3)	8326 (4)
P(1)	−1549 (2)	1773 (1)	5829 (1)	C(42)	−1694 (7)	701 (3)	8943 (4)
P(2)	924 (2)	415 (1)	7831 (1)	C(43)	−3199 (9)	601 (4)	9197 (5)
O(1)	−635 (6)	522 (2)	4239 (3)	C(44)	−4051 (8)	112 (4)	8813 (5)
O(2)	−2117 (9)	2775 (4)	3788 (5)	C(45)	−3370 (8)	−258 (3)	201 (5)
O(3)	2614 (5)	2126 (2)	5922 (3)	C(46)	−1849 (8)	−167 (3)	7966 (5)
O(4)	1878 (6)	1862 (3)	2986 (3)	C(5a)	−1352	1391	7336
C(1)	—461 (7)	1025 (3)	4384 (4)	H(5b)	198	1742	7143
C(2)	−1315 (7)	2397 (3)	4184 (4)	H(6a)	−481	585	6399
C(3)	1581 (7)	2014 (3)	5402 (4)	H(6b)	1144	923	6411
C(4)	1129 (7)	1847 (3)	3627 (4)	H(12)	−3442	957	6935
C(5)	−571 (6)	1456 (2)	6892 (4)	H(13)	−5741	370	6600
C(6)	242 (10)	842 (4)	6760 (5)	H(14)	−6974	384	5131
C(11)	−3352 (5)	1320 (2)	5632 (4)	C(15)	−6054	1005	3963
C(12)	−3965 (7)	967 (2)	6321 (4)	H(16)	−3690	1565	4260
C(13)	−5324 (7)	620 (3)	6125 (5)	H(22)	−4341	2239	6668
C(14)	−6053 (7)	630 (3)	5258 (5)	H(23)	−4989	3194	7334
C(15)	−5493 (7)	987 (3)	4566 (4)	H(24)	−3277	4018	7276
C(16)	−4124 (9)	1328 (4)	4744 (6)	H(25)	−926	3909	6561
C(21)	−2216 (6)	2513 (2)	6251 (3)	H(26)	−255	2978	5897
C(22)	−3625 (6)	2577 (3)	6656 (4)	H(32)	2862	1430	7451
C(23)	−4019 (7)	3147 (3)	7036 (4)	H(33)	4439	2134	8327
C(24)	−3010 (7)	3633 (3)	7007 (4)	H(34)	4693	2016	9979
C(25)	−1628 (7)	3568 (3)	6589 (4)	H(35)	2884	1432	10679
C(26)	−1217 (7)	3018 (3)	6206 (4)	H(36)	1463	682	9834
C(31)	1957 (6)	998 (3)	8540 (4)	H(42)	−1068	1013	9255
C(32)	2894 (9)	1418 (4)	8121 (6)	H(43)	−3655	881	9618
C(33)	3866 (7)	1822 (3)	8630 (4)	H(44)	−5101	35	8988
C(34)	3902 (8)	1807 (3)	9593 (5)	H(45)	−3967	−582	7900
C(35)	2998 (8)	1391 (3)	10021 (4)	H(46)	−1372	−437	7540
C(36)	2056 (10)	980 (4)	9512 (6)				

= 5.47%, R_{wF} = 5.49%, and GOF = 1.03 for those 2693 unique relections with $|F_o| > 2\sigma(|F_o|)$. The largest peak in a final difference Fourier synthesis was 0.48 e Å^{-3} and was located 1.14 Å from P(2).

Final positional parameters are given in Table II. A listing of observed vs. calculated structure factors and anisotropic thermal parameters are available as supplementary material.

Results and Discussion

Synthesis. The synthesis and isolation of a unidentate diphos complex require a reaction pathway that inhibits chelation. Complexes that are inherently labile or those that readily increase their coordination number are unlikely candidates. Substitution of PPh_3 for CO in $Fe(CO)_4PPh_3$ has been shown to proceed by an S_N1 mechanism and has a very high free energy of activation.[20] It is, therefore, expected that $Fe(CO)_4(\eta^1$-diphos) and $Fe(CO)_3(\eta^1$-diphos$)_2$ would be quite stable with respect to chelation. The prediction is borne out in this work. The addition of PPh_2H to $Fe(CO)_{5-n}(PPh_2CH{=}CH_2)_n$ (n = 1 or 2) is promoted by potassium *tert*-butoxide.

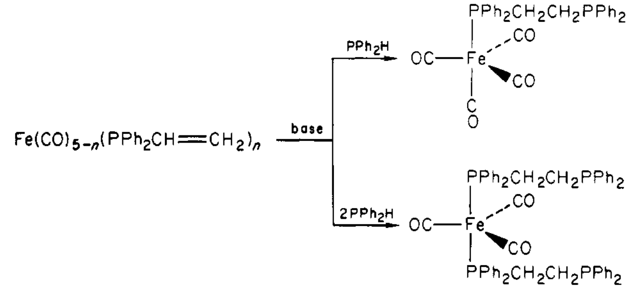

As with vinylphosphine complexes of group 6, the addition of secondary phosphine may also be promoted by the free radical catalyst AIBN. Of the two methods we prefer base promotion because reasonable yields are consistently obtained. In general the iron complexes are obtained in lower yields than the corresponding group 6 complexes. The iron complexes are quite stable in the solid state, and in fact $Fe(CO)_4(\eta^1$-disphos), which melts at 131 °C, does not visibly lose CO until temperatures exceed 180 °C. While unidentate diphos complexes of group 6 can be prepared from coordinated secondary phosphines in basic medium, we have not been successful in adding $Fe(CO)_4(PPh_2H)$ or $Fe(CO)_3(PPh_2H)_2$ to $PPh_2CH{=}CH_2$ by either base or free radical promotion.

Vinyl addition reactions provide an approach to synthesizing mixed-metal complexes containing bridging diphos. We have reported previously the syntheses of $(OC)_5MPPh_2CH_2CH_2PPh_2M'(CO)_5$ (M ≠ M' = Cr, Mo, W)[21] and $(OC)_5CrPPh_2CH_2CH_2PPh[W(CO)_5]CH_2CH_2PPh_2Mo(CO)_5$[22] from judiciously selected coordinated precursors of diphos. Similarly we now find that diphos readily bridges $-Fe(CO)_4$ and $-W(CO)_5$.

$$Fe(CO)_4(PPh_2CH{=}CH_2) + W(CO)_5PPh_2H \xrightarrow{\text{base}} (OC)_4FePPh_2CH_2CH_2PPh_2W(CO)_5$$

Structure Description. Selected bond distances and angles with estimated deviations are shown in Table III. The molecular geometry and numbering scheme are shown in Figure 1; a stereoview is provided in Figure 2. The title compound crystallizes in discrete, well-separated molecules. The geometry about the Fe atom is trigonal bipyramidal, with three equatorial and one axial carbonyl groups. The three equatorial carbon atoms tilt slightly toward the coordinated phosphorus group. This structural feature has been observed and accounted for in many other axially substituted ML_4L' complexes.[23] The diphos ligand is axially bonded to iron through P(1) exclusively. The Fe···P(2) distance, 4.553 (2) Å, precludes any meaningful association. Although phosphines exhibit little basicity toward coordinated CO, the possibility of the dangling phosphorus group experiencing some interaction with carbon in the solid state was intriguing. Weak interactions of nucleophiles with bound CO groups appear to be mechanistically important in a number of systems,[24] but for the d^8 $Fe(CO)_4(\eta^1$-diphos) complex, the electron-rich d orbitals that reside between the ligands undoubtedly repel the lone pair of the dangling phosphorus group. The phosphorus atoms are trans with the two diphenylphosphino groups gauche to one another with a dihedral angle of 43° relating the C(11)–C(21) plane to the C(31)–C(41) plane. The average C–P–C bond angle for the coordinated phosphorus group is 0.9° larger than for the uncoordinated phosphorus group, a result which is expected but not statistically significant.

Table III. Selected Bond Distances and Angles with Esd's for $(CO)_4Fe[(C_6H_5)_2PCH_2]_2$

(a) Bond Distances (Å)

Fe–P(1)	2.246 (2)	Fe–C(4)	1.771 (6)
Fe···P(2)	4.553 (2)	C(1)–O(1)	1.135 (7)
Fe–C(1)	1.792 (6)	C(2)–O(2)	1.147 (9)
Fe–C(2)	1.788 (6)	C(3)–O(3)	1.143 (7)
Fe–C(3)	1.791 (6)	C(4)–O(4)	1.153 (8)

(b) Bond Angles (deg)

C(1)–Fe–P(1)	88.7 (2)	Fe–C(1)–O(1)	178.1 (6)
C(2)–Fe–P(1)	88.9 (2)	Fe–C(2)–O(2)	179.1 (6)
C(3)–Fe–P(1)	88.0 (2)	Fe–C(3)–O(3)	178.4 (5)
C(4)–Fe–P(1)	179.3 (2)	Fe–C(4)–O(4)	179.2 (5)
C(1)–Fe–C(2)	120.6 (3)	Fe–P(1)–C(5)	114.7 (2)
C(1)–Fe–C(3)	118.8 (3)	Fe–P(1)–C(11)	114.7 (2)
C(1)–Fe–C(4)	90.8 (3)	Fe–P(1)–C(21)	115.3 (2)
C(2)–Fe–C(3)	120.5 (3)	P(1)–C(5)–C(6)	114.6 (4)
C(2)–Fe–C(4)	91.0 (3)	P(2)–C(6)–C(5)	117.3 (5)
C(3)–Fe–C(4)	92.6 (3)		

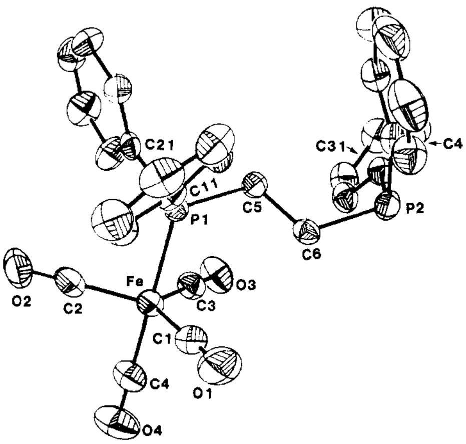

Figure 1. Drawing of an individual molecule of $Fe(CO)_4(\eta^1$-$Ph_2PCH_2CH_2PPh_2)$ showing the labeling scheme. Vibrational ellipoids are drawn at the 50% probability level.

For d^8 trigonal-bipyramidal geometry, symmetry and overlap arguments indicate that better σ donors will occupy axial sites while better π acceptors will occupy equatorial

---

(20) Siefert, E. E.; Angelici, R. J. *J. Organomet. Chem.* **1967**, *8*, 374. Modi, S. P.; Atwood, J. D. *Inorg. Chem.* **1983**, *22*, 26.

(21) Keiter, R. L; Kaiser, S. L.; Hansen, N. P.; Brodack, J. W. *Inorg. Chem.* **1981**, *20*, 283.

(22) Keiter, R. L.; Borger, R. D.; Madigan, M. J.; Kaiser, S. L.; Rowley, D. L. *Inorg. Chem. Acta* **1983**, 76, L5.

(23) Riley, P. E.; Davis, R. E. *Inorg. Chem.* **1980**, *19*, 159.

(24) Brown, T. L.; Bellus, P. A. *Inorg. Chem.* **1978**, *17*, 3726.

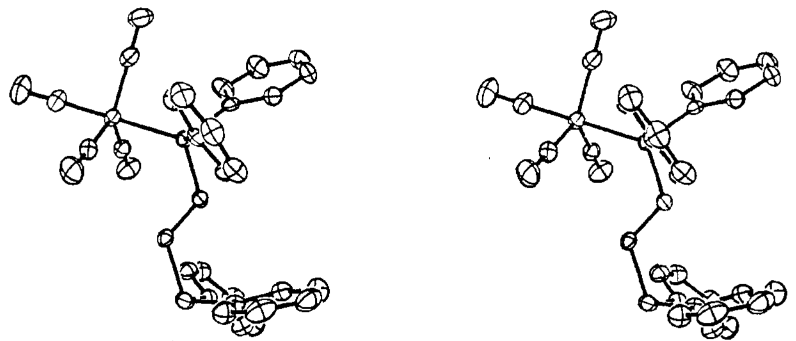

Figure 2. Stereoscopic view of $Fe(CO)_4(\eta^1\text{-}Ph_2PCH_2CH_2PPh_2)$.

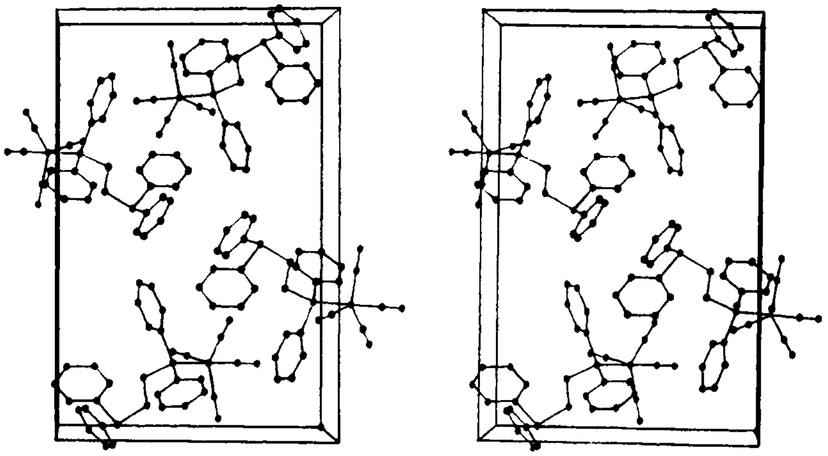

Figure 3. Stereoscopic view of the unit cell of $Fe(CO)_4(\eta^1\text{-}Ph_2PCH_2CH_2PPh_2)$.

Table IV. Some Bond Lengths (Å) in Axial $Fe(CO)_4$(phosphine) Compounds

	ligand					
bond	$[CH_3NCH_2CH_2N(CH_3)PF$[30]	$Ph_2PC{=}C(AsMe_2)CF_2CF_2$[31]	PPh_3[23]	η^1-diphos	PPh_2H[32]	P-*t*-Bu_3[28]
Fe-P	2.174 (1)	2.224 (3)	2.244 (1)	2.246 (2)	2.237 (2)	2.364 (1)
Fe-CO(ax)	1.798 (6)	1.74 (2)	1.795 (4)	1.771 (6)	1.792 (8)	1.768 (8)

sites.[25] Thus phosphines are almost invariably axially located while olefins are found in equatorial positions.[26] Bulky ligands, from steric considerations, would be expected to coordinate equatorially but only rarely do steric factors override electronic considerations. In spite of a cone angle[27] of 179° for P-*t*-Bu_3, the ligand is found axially bound in $Fe(CO)_4P$-*t*-Bu_3.[28] Equatorial substitution is found in $Fe(CO)_4[PPh(PPh_2)_2]$ which contains a ligand whose space requirement is extreme.[29] From these considerations, it is seen that both electronic and steric factors favor axial diphos.

The carbon–oxygen bond length (1.153 (8) Å) of the carbonyl group coaxial with the diphos group is slightly longer than that of the average equatorial carbonyl group, (1.142 (8) Å), as is expected from the effects of increased d–π^* back-donation to the carbonyl group. A related effect is seen in the shortening of the carbon–metal bond coaxial with the phosphorus–metal bond, 1.771 (6) vs. 1.790 (6) Å (av).

Table IV compares Fe–P and $Fe{-}CO_{(axial)}$ bond lengths for a series of axially substituted phosphines. The longest observed Fe–P bond (2.364 Å) is found in $Fe(CO)_4P$-*t*-Bu_3, but in this example steric interaction between the phosphorus and cis CO groups leads to an abnormally long bond. The shortest Fe–P bond (2.174 Å) is found in the fluoro phospholidine complex[30] in which the ligand is expected to be a good π acceptor. The $Fe{-}CO_{(axial)}$ bond lengths of these two complexes are consistent with Fe–P bond lengths in that the longest metal–carbon bond is found for the phospholidines and the shortest for P-*t*-Me_3. The phenyl-substituted phosphine ligands have similar Fe-P bond lengths as well as $Fe{-}CO_{(axial)}$ bond lenths and neither form an easily rationalized series.

Spectroscopic Studies. The number and intensities of carbonyl stretching absorptions in the infrared spectrum of $Fe(CO)_4L$ complexes have been used by many workers to draw conclusions about axial vs. equatorial substitution.[33] Axial C_{3v} symmetry requires three active infrared stretching modes (2A + E), but in practice many axial phosphines sufficiently lower the symmetry of the complex to give four absorptions. Since equatorial C_{2v} symmetry gives rise to four absorptions also, differentiation between

---

(25) Rossi, A. R.; Hoffman, R. *Inorg. Chem.* **1975**, *14*, 365.

(26) Stainer, M. V. R.; Takats, J. *Inorg. Chem.* **1982**, *21*, 4044.

(27) Tolman, C. A. *J. Am. Chem. Soc.* **1970**, *92*, 2956.

(28) Pichardt, J.; Rosch, L.; Schumann, H. *J. Organomet. Chem.* **1976**, *107*, 241.

(29) Sheldrick, W. S.; Morton, S.; Stelzer, O. *Z. Anorg. Allg. Chem.* **1981**, 475, 232.

(30) Bennett, D. W.; Neustadt, R. J.; Parry, R. W.; Cagle, F. W. *Acta Crystallogr., Sect. B* **1978**, *B34*, 3362.

(31) Einstein, F. W. B.; Jones, R. D. G. *J. Chem. Soc., Dalton Trans.* **1972**, 442.

(32) Kilbourn, B. T.; Raeburn, U. A.; Thompson, D. T. *J. Chem. Soc. A* **1969**, 1906.

(33) Darensbourg, D. J. *Inorg. Chim. Acta* **1970**, *4*, 597.

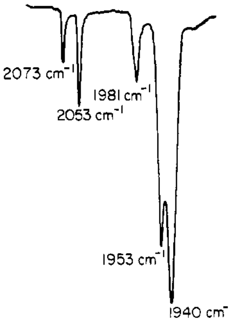

Figure 4. Infrared spectrum of the carbonyl stretching region of $(OC)_4FePPh_2CH_2CH_2PPh_2W(CO)_5$.

the two structures cannot be made with certainty only by counting bands. However, by considering both the number and intensities of the absorptions, the correct structure can usually be predicted. Both $Fe(CO)_4(\eta^1$-diphos) and $Fe(CO)_4(\eta^1-PPh_2CH_2PPh_2)$ give rise to four absorptions in C_6H_{12} and have intensities characteristic of axial substitution. The infrared spectrum of $(OC)_4FePPh_2CH_2CH_2PPh_2W(CO)_5$ in the carbonyl region is a superimposition of patterns characteristic of local C_{3v} and C_{4v} symmetries at Fe (2053, 1981, 1953 cm^{-1}) and W (2073, 1940 cm^{-1}) carbonyl moieties, respectively (Figure 4).

The $^{31}P\{^1H\}$ spectrum of $Fe(CO)_4(\eta^1$-diphos) consists of two doublets with the uncoordinated phosphorus resonance unshifted from the free ligand while the coordinated phosphorus signal is found downfield at 68.1 ppm. The phosphorus–phosphorus coupling (40.2 Hz) is typical of monocoordinated diphos.[7,34,35] The $^{31}P\{^1H\}$ NMR spectrum of axial $Fe(CO)_4(\eta^1-PPh_2CH_2PPh_2)$ also shows two doublets with the uncoordinated phosphorus shifted 4 ppm upfield (−25.7 ppm) and the downfield signal arising from the coordinated phosphorus (65.9 ppm). The phosphorus–phosphorus coupling is of special significance. Equatorial $Fe(CO)_4(\eta^1-PPh_2CH_2PPh_2)$ has been postulated from NMR and IR evidence, though not isolated, as a product of the reaction of $Fe(PPh_2CH_2PPh_2)_2(C_2H_4)$ and CO.[36] Chemical shifts ascribed to this species, 74.5 and −27.2 ppm, are not unreasonable, but the reported value of 25 Hz for $^2J_{PP}$ differs by 50 Hz from that for our axial species. It is unlikely that the magnitude of the coupling would change so dramatically as a result of the geometrical difference between axial and equatorial isomers.[37] The reported coupling may be more consistent with a low-spin Fe(II) complex.[10]

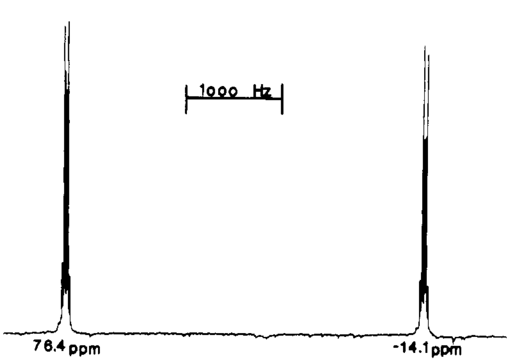

Figure 5. $^{31}P\{^1H\}$ spectrum of *trans*-$Fe(CO)_3(\eta^1-Ph_2PCH_2CH_2PPh_2)_2$.

Few complexes containing two unidentate diphos complexes have been synthesized.[7,9,10] The AA′XX′ spin system that arises from $Fe(CO)_3(\eta^1$-diphos$)_2$ gives a spectrum (figure 5) that allows $^2J_{PP}$ to be obtained directly.[7] The coupling of phosphorus groups trans to one another is often large but in this case, as in *trans*-$Cr(CO)_4(\eta^1$-diphos$)_2$ (26.0 Hz), a small value is observed (30.4 Hz). This is in contrast to the reported ruthenium porphyrin phosphine complexes in which $^2J_{PP}$ is sufficiently large to create virtually coupled specta.[10]

Two doublets are observed in the $^{31}P\{^1H\}$ NMR spectrum of $(OC)_4FePPh_2CH_2CH_2PPh_2W(CO)_5$, and the one possessing tungsten-183 satellites identifies the tungsten–phosphorus absorption. The chemical shifts and coupling constants are not unusual.

Acknowledgment is made to the donors of the Petroleum Research Fund, administered by the American Chemical Society, for support of this research, to the NSF Regional Center at the University of Illinois (NSF CHE 79-16100), and to Ellen A. Keiter for helpful discussions.

Registry No. $Fe(CO)_4PPh_2CH{=}CH_2$, 87137-60-8; $Fe(CO)_4(\eta^1-PPh_2CH_2PPh_2)$, 52843-12-6; *trans*-$Fe(CO)_3(PPh_2CH{=}CH_2)_2$, 87137-61-9; $Fe(CO)_4(\eta^1-PPh_2CH_2CH_2PPh_2)$, 87137-62-0; $Fe(CO)_3(\eta^1-PPh_2CH_2CH_2PPh_2)_2$, 87137-63-1; $(OC)_4FePPh_2CH_2CH_2PPh_2W(CO)_5$, 87137-64-2.

Supplementary Material Available: A full crystallographic report including tables of positional and thermal parameters, atomic coordinates and temperature factors, bond lengths, bond angles, hydrogen coordinates and temperature factors, and structure factor amplitudes (20 pages). Ordering information is given on any current masthead page.

---

(34) Keiter, R. L.; Cary, L. W. *J. Am. Chem. Soc.* **1972**, *94*, 9232

(35) Colquhoun, I. J.; McFarlane, W. *J. Chem. Soc. Dalton Trans.* **1982**, 1915.

(36) Ittel, S. D.; Tolman, C. A.; Krusic, P. J.; English, A. D.; Jesson, J. P. *Inorg. Chem.* **1978**, *17*, 3432.

(37) A conformational change within the ligand could account for the coupling constant difference. Large variations in $^2J_{PP}$ have been noted in X_2PNRPX_2. Keat, R.; Manojlović-Muir, L.; Muir, K. W.; Rycroft, D. S. *J. Chem. Soc., Dalton Trans.* **1981**, 2192.